

Structure, barriers and relaxation mechanisms of kinks in the 90° partial dislocation in silicon

R. W. Nunes, J. Bennetto, and David Vanderbilt

Department of Physics and Astronomy, Rutgers University, Piscataway, NJ 08855-0849

(October 31, 2018)

Kink defects in the 90° partial dislocation in silicon are studied using a linear-scaling density-matrix technique. The asymmetric core reconstruction plays a crucial role, generating at least four distinct kink species as well as soliton defects. The energies and migration barriers of these entities are calculated and compared with experiment. As a result of certain low-energy kinks, a peculiar alternation of the core reconstruction is predicted. We find the solitons to be remarkably mobile even at very low temperature, and propose that they mediate the kink relaxation dynamics.

61.72.Lk, 71.15.Pd, 71.15.Fv

The importance of dislocations in semiconductors hardly needs comment. In addition to being responsible for plastic behavior in general, dislocations occur commonly at semiconductor interfaces where they can act as trapping and scattering centers for carriers. In silicon, the predominant slip system consists of 60° -edge and screw dislocations oriented along $\langle 110 \rangle$ and lying in a $\{111\}$ slip plane. Both are known to dissociate into pairs of partial dislocations bounding a ribbon of stacking fault [1]. The resulting 90° or 30° partial dislocations are believed to have reconstructed cores, consistent with the low density of dangling bonds as observed by EPR measurements [1]. Since the dislocation motion occurs by nucleation and propagation of kinks along the dislocation line, a detailed understanding of the atomic-scale structure of the kinks is obviously of the greatest importance. Unfortunately, experimental approaches have not proved capable of providing such an understanding.

Until recently, the only theoretical methods capable of treating such problems were based on classical interatomic potentials. These are of questionable accuracy, and are generally unable to reproduce effects of intrinsic quantum-mechanical nature such as bond reconstruction and Peierls or Jahn-Teller symmetry breaking. For example, while the Stillinger-Weber [2] potential has been used to study the core reconstruction and kinks of the 30° partial [3], it fails to reproduce the correct core reconstruction of the 90° partial [4]. It is thus exciting to find that *ab-initio* methods are approaching the point of addressing some interesting questions about dislocations. Recent theoretical work has focused on such issues as the core reconstruction of the 90° [4,5], and the elastic interaction between dislocations of a dipole in the shuffle [6] and glide [5] sets. One first-principles study has even been done on a kink barrier in the 30° partial, [7] but it assumed a kink structure previously proposed, and used a relatively small supercell. Cluster calculations on the 90° partial have also been reported [8]. However, a com-

prehensive study of dislocation kink structure and dynamics would require the use of very large supercells, for which the application of *ab-initio* techniques is still computationally prohibitive. Thus, there is a pressing need for the application of more efficient quantum-mechanics based methods to study the electronic and structural excitations in this system.

In this Letter, we use a total-energy tight-binding (TBTE) description of the electronic and interatomic forces to carry out a detailed atomistic study of this kind for the 90° partial dislocation in silicon. The key to making the calculations tractable is our use of a “linear-scaling” or “ $\mathcal{O}(N)$ ” method of solution of the Schrödinger equation [9], enabling us to treat system sizes up to 10^3 atoms easily on a workstation platform. We verify that the dislocation core reconstructs with a spontaneous symmetry breaking, and find that the “soliton” defect associated with the reversal of the core reconstruction is extremely mobile. We find that at least four distinct kink structures must be considered (labeled by the sense of the core reconstruction on either side), and show that they can be classified as high- or low-energy kinks depending on whether or not they contain a dangling bond. Molecular-dynamics simulations as well as fully-relaxed static calculations are used to characterize formation energies, migration barriers, and kink-soliton reaction pathways. The picture that emerges is one in which the ground state is free of dangling bonds (even in the presence of kinks), and in which the solitons mediate the structural excitations and dynamics.

We use the TBTE parameters of Kwon *et al.* [10], with a real-space cutoff of 6.2\AA on the range of the density matrix used in the $\mathcal{O}(N)$ method [9]. We chose to work at a fixed electron chemical potential 0.4 eV above the valence-band edge, and thus all “energies” reported below are technically values of grand potential [9]. The numerical minimization of the $\mathcal{O}(N)$ functional was carried out by the conjugate-gradient algorithm, with the inter-

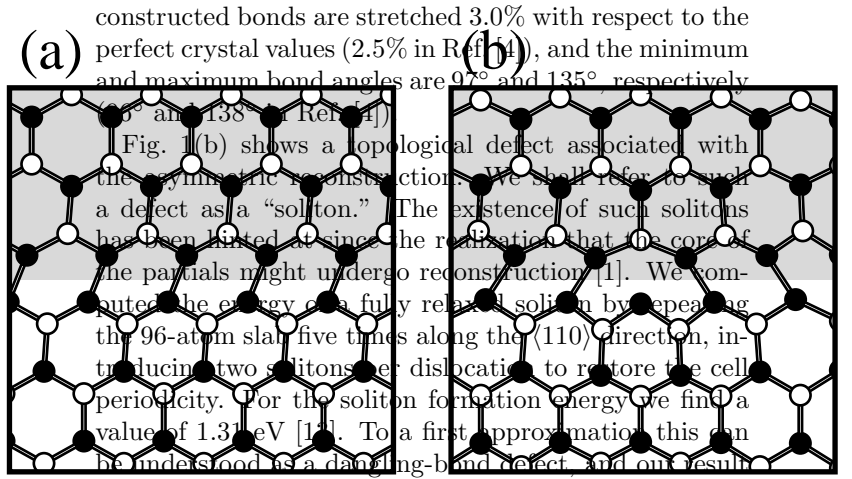


FIG. 1. (a) Top view of the slip plane of a reconstructed 90° partial dislocation. The shaded area indicates the stacking fault. Horizontal and vertical directions correspond to $[1\bar{1}0]$ and $[11\bar{2}]$ directions, respectively. (b) Reconstruction defect, or soliton, where the core reconstruction changes orientation.

nal line minimization performed exactly [11]. Ground-state structures were computed by allowing all atomic coordinates to relax fully (forces less than 5 meV/Å). The supercells used will be described below; all energies for defect (soliton and kink) structures are given with respect to a corresponding supercell containing defect-free (but reconstructed and fully relaxed) dislocations. Barrier energies were calculated by choosing a reaction coordinate and, for a series of values of this coordinate, computing the energy with this coordinate fixed and all others fully relaxed. Molecular dynamics runs were performed with a Verlet algorithm, the Nose thermostat [12], and a time step of 2 fs.

In Fig. 1(a), a top view of the atomic structure of the reconstructed 90° partial in its slip plane is shown. The shaded area indicates the stacking fault. The fourfold coordination of the atoms at the core is restored by bonding across the dislocation line. This reconstruction has been discussed by other authors [4,5] and compared with an alternative “quasi-fivefold” bond reconstruction that preserves the mirror symmetries along the dislocation line. As a test of our TBTE-DM approach, we computed the energy difference between the two possibilities. In this calculation the supercell consisted of a 96-atom slab normal to a $\langle 110 \rangle$ direction, containing two dislocations with opposite burgers vectors separated by a distance of 13.3 Å. We find the fourfold reconstruction to be 0.18 eV/Å lower in energy than the fivefold one, in perfect agreement with the TB calculations in Ref. [5]. Our results also compare favorably with the *ab initio* results in Ref. [4], for which the energy difference between the two reconstructions is 0.23 eV/Å. In our calculations, the re-

is on the order of the energy associated with a dangling sp^3 orbital in silicon.

An interesting question is whether a soliton can move easily along the dislocation. We computed an energy barrier of only 0.04 eV for the propagation of a soliton between two adjacent equilibrium positions, as indicated in Fig. 1(b). With such a small barrier, it might be expected that the solitons would be extremely mobile even at very low temperatures. To test this, we performed a molecular dynamics simulation on a supercell having a soliton-antisoliton pair, initially separated by 9.6 Å, on an otherwise defect-free partial dislocation. Remarkably, at a temperature of only 50 K°, the solitons were indeed mobile and recombination of the pair took place after only 1.3 ps. Such highly mobile solitons play an interesting role in the relaxation of high-energy kinks, as explained below.

A schematic view of the supercell we used for simulating kinks and soliton-kink complexes is shown in Fig. 2. It contains a total of 864 atoms, corresponding to the 96-atom slab repeated nine times along the dislocation line ($[1\bar{1}0]$ direction). The supercell vectors and the crystalline directions are indicated. In Figs. 3(a)-(e) the local structures of the five different types of kinks are displayed. The notation we chose to name each kink type is related to the orientation of the reconstructed bond, as one moves from left to right in each diagram in Fig. 3. For example, in Fig. 3(a) we denote the orientation at the left of the kink as “right” (R). Hence, we call this a right-left (RL) kink, the notation following accordingly for the other types. The above supercell was used to compute the energies for the LR and RL kinks. The lattice vector was staggered by twice the “kink vector” [14], as shown in Fig. 2, in order to accommodate one RL and one LR kink in each dislocation. Fig. 3(f) shows a complex of a LR kink and a soliton. For the configurations in Figs. 3(c)-(f) the bonds on either side of the defect have the same orientation. For these, a supercell of 432 atoms was used (half of that shown in Fig. 2), having one kink or complex in each dislocation, with a supercell vector staggered by one kink vector.

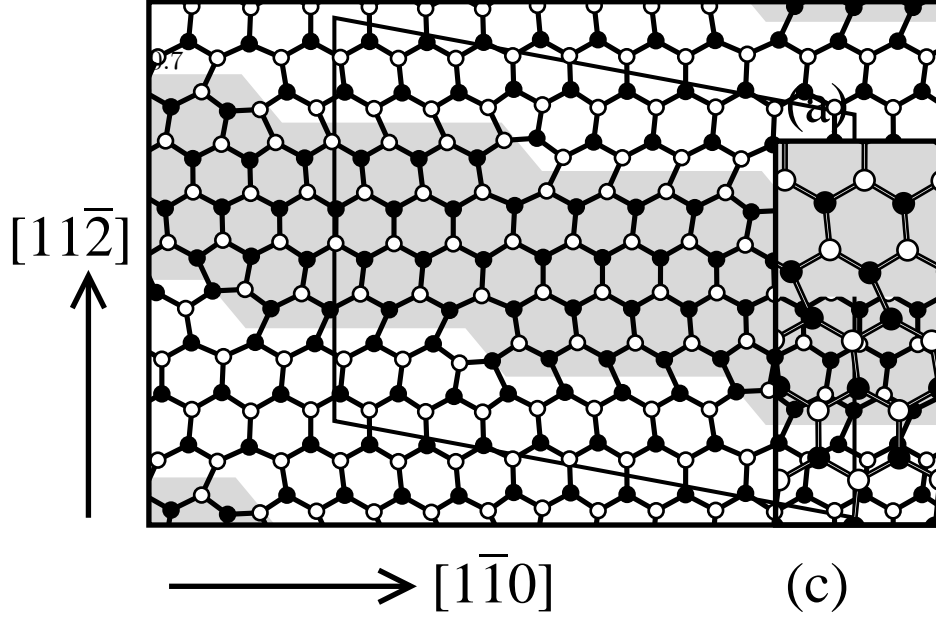


FIG. 2. Supercell used for kinks and kink-soliton complexes. Crystalline directions and supercell vectors indicated. Unit cell contains 864 atoms.

Our results for the energies of the configurations in Fig. 3 are shown in Table I. It is seen that the LR and RL kinks are much lower in energy than all the others. (The LL and LL* kinks are found to be unstable against emission of a soliton, a mechanism that is discussed in detail in the next paragraph.) An inspection of Fig. 3 shows that the LR and RL kinks are fully reconstructed, with no dangling bonds. On the other hand, the high-energy RR kink and the unstable LL kinks all contain a dangling bond (note the three-fold coordinated atom at the core of each defect). This distinction is clearly responsible for most of the energy difference. On the basis of the energetics alone, we can thus conclude that any kinks which occur in the 90° partial dislocation in silicon will be almost entirely of type LR or RL. This means that the orientation of the core reconstruction is predicted to alternate from one inter-kink segment to the next along the dislocation.

Moreover, we see that the RL + S and LR + S complexes (S = soliton) have lower energies than the RR and LL kinks. From the energetics in Table I we can write the following reaction equations:

$$RR \rightarrow RL + S + 0.41 \text{ eV}; \quad (1)$$

$$RR \rightarrow LR + S + 0.36 \text{ eV}; \quad (2)$$

$$LL \rightarrow LR + S \text{ (spontaneous)}; \quad (3)$$

$$LL^* \rightarrow RL + S \text{ (spontaneous)}. \quad (4)$$

Reactions (1) and (2) above consists of the emission of a soliton by the RR kink, which turns into a LR or RL in the process. We estimated the energy barrier for these

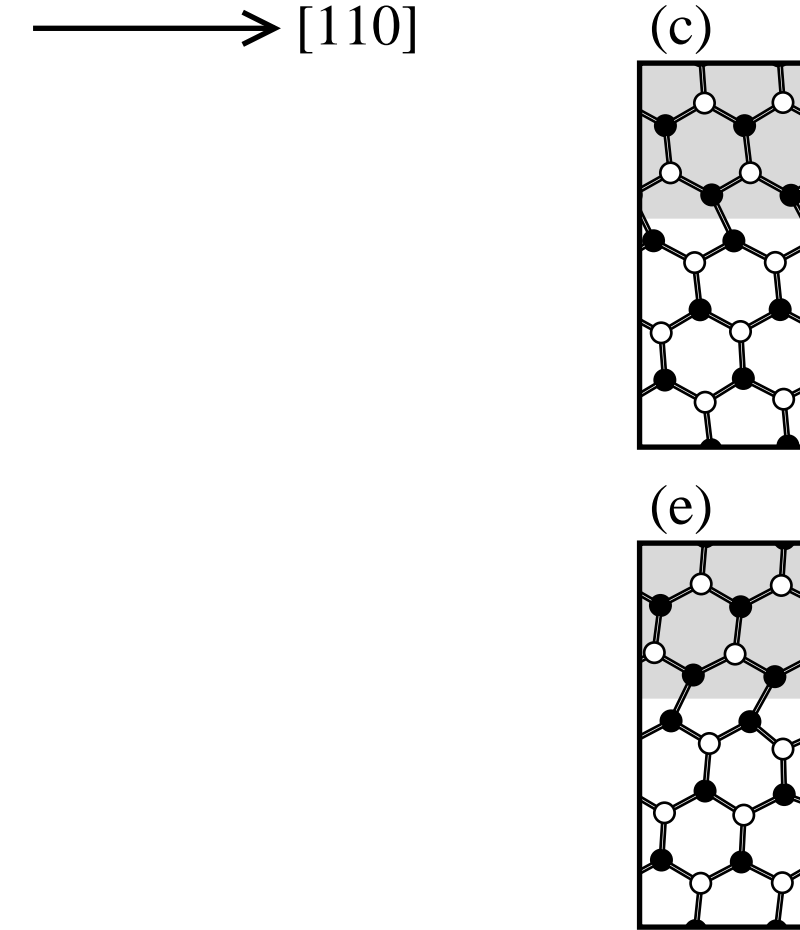


FIG. 3. Core structure of various kinks and a kink-soliton complex. Kink notation relates to bond reconstruction on each side of the defect, and is explained in the text. (a) RL kink. (b) LR kink. (c) LL kink. (d) LL* kink. (e) RR kink. (f) LR kink + soliton.

TABLE I. Calculated formation energy for defects in the core of the 90° partial dislocation in silicon. Included also are the migration barriers for a soliton and the low energy kinks.

	Formation energy (eV)	Migration barrier (eV)
soliton	1.31	0.04
LR kink	0.50	1.87
RL kink	0.50	1.83
LL kink ^a	1.74	—
LL* kink ^a	1.76	—
RR kink	2.04	—
soliton + LR kink	1.68	—
soliton + RL kink	1.63	—

^aApproximate energy. Defect is unstable

processes, obtaining the value of 0.05 eV. This result is not surprising in view of the low energy barrier for soliton motion. The same mechanism is involved in the instability of the LL and LL* kinks. Here the asymmetry of the local strain fields is enough to remove the barrier to emission of the soliton in one direction.

We decided to put the above picture to test by performing a MD simulation on a 864-atom supercell containing four RR kinks, two in each dislocation. Thus it should be possible for the system to convert these kinks into alternating LR and RL kinks, as is to be expected from the energetics in Table I. At room temperature a RR kink in one of the dislocations emitted a soliton after 0.2 ps, turning into a RL kink. This soliton propagated towards the other RR kink in the same dislocation and fused with it (converting it to a LR kink) after only 0.7 ps. The latter process is equivalent to recombination of the propagating soliton with an anti-soliton “embedded” in the RR kink.

In Table I, we also include the energy barriers to motion of the RL and LR kinks. For metals, the formation of double kinks controls the rate of dislocation motion, and the energy barriers to kink propagation along the dislocation line are very small. The high values we obtained for silicon are a signature of the highly directional bonds in covalent semiconductors. In these systems, dislocation motion is believed to be controlled by the kink mobility. Recent experiments [15,16] have confirmed this picture, but some controversy still remains, and the role of impurities as obstacles to kink motion is yet to be fully explored. Here we concentrate on the important issue of the size of the kink formation energies and migration barriers, and make a connection with the experimental results. For the velocity of a gliding dislocation we have, from the theory of Ref. [17]

$$v_d \propto \exp[-(U_k + W_m)/kT], \quad (5)$$

where U_k is the formation energy of a kink and W_m is the energy barrier for kink migration along the dislocation. The experimental estimates based on transmission

electron microscopy (TEM) or intermittent loading (IL) measurements [15,16] range from 0.40 to 0.62 eV for U_k and 1.50 to 1.80 eV for W_m . Our results from Table I, $U_k = 0.50$ eV and $W_m = 1.85$ eV (average between LR and RL values), fall within the range of the experimental numbers. The theory in Ref. [17] can be used to calculate the Peierls stress of materials. When the above numbers are used for silicon, one obtains a value that is too low in comparison with results of high-stress measurements. Discrepancies are also found for quantities such as the velocity of steady-state motion of a dislocation under static load [16]. It has been argued in Ref. [16] that these discrepancies are to be assigned to point defects that would influence both the concentration of kinks and their migration barriers, by creating inhomogeneities in the potential relief (the potential felt by a moving dislocation due to the periodicity of the lattice). The above comparison between experiment and our results, which are valid for a homogeneous potential relief, reinforces the plausibility of this scenario.

In summary, we investigated different structural and dynamical properties of the 90° partial dislocation in silicon. We verified that the core undergoes a reconstruction that breaks the mirror symmetry along the dislocation line, as previously reported. This leads to the existence of solitons which are shown to be highly mobile along the dislocation core, and to a multiplicity of kinks whose stability is found to depend, in each case, on the reconstruction of dangling bonds at the core of the defect. We find that the high-energy kinks transform into low-energy ones by soliton emission. The energy barriers associated with this mechanism are small or absent in each case. The low-energy kinks are fully reconstructed with no dangling bonds, and impose an alternation of the orientation of the core reconstruction from one inter-kink segment to the next. The mobility of these low-energy kinks presumably determines the dislocation mobility in the glide plane. Our calculated formation energies and energy barriers for these kinks are in good agreement with available experimental estimates.

During the final stages of preparation of this manuscript, we became aware of related work by Hansen *et al.* [18], who consider some similar kink structures but with a much smaller interkink separation than was considered here.

This work was supported by NSF Grant DMR-91-15342. R. W. Nunes acknowledges the support from CNPq - Brazil. J. Bennetto acknowledges support of ONR Grant N00014-93-I-1097.

[1] P. B. Hirsch, Mater. Sci. Tech. **1**, 666 (1985)

- [2] F. H. Stillinger and T. A. Weber, Phys. Rev. A **25**, 978 (1985).
- [3] V. V. Bulatov, S. Yip, and A. S. Argon, Philos. Mag. A **72**, 453 (1995).
- [4] J. R. K. Bigger *et al.*, Phys. Rev. Lett. **69**, 2224 (1992).
- [5] L. B. Hansen *et al.*, Phys. Rev. Lett. **75**, 4444 (1995).
- [6] T. A. Arias and J. D. Joannopolous, Phys. Rev. Lett. **73**, 680 (1994).
- [7] Y. M. Huang, J. C. Spence, and O. F. Sankey, Phys. Rev. Lett. **74**, 3392 (1995).
- [8] M.I. Heggie, R. Jones, and A. Umerski, Phys. Stat. Sol. (a) **138**, 383 (1993).
- [9] X.-P. Li, R. W. Nunes, and D. Vanderbilt, Phys. Rev. B **47**, 10891 (1993).
- [10] I. Kwon *et al.*, Phys. Rev. B **49**, 7242 (1994).
- [11] Because the functional is exactly a cubic polynomial, its minimum can be located immediately by evaluating its value and first three derivatives at any single point on the line.
- [12] S. Nosé, Prog. Theor. Phys. Suppl. **103**, 1 (1991).
- [13] This is in reasonable agreement with the estimate of 1.2 eV obtained in Ref. [8] from a $\text{Si}_{34}\text{H}_{39}$ cluster calculation.
- [14] A “kink vector” is the vector by which a dislocation shifts between two neighboring Peierls valleys. It relates equivalent atoms in adjacent sub-layers of the diamond lattice.
- [15] H. Gottschalk *et al.*, Phys. Stat. Sol. (a) **138**, 547 (1993).
- [16] B. Ya. Farber, Yu. L. Iunin, and V. I. Nikitenko, Phys. Stat. Sol. (a) **97**, 469 (1986); V. I. Nikitenko, B. Ya. Farber, and Yu. L. Iunin, Sov. Phys. JETP **66**, 738 (1987); B. Ya. Farber *et al.*, Phys. Stat. Sol. (a) **138**, 557 (1993).
- [17] J. P. Hirth and J. Lothe, *Theory of Dislocations*, (Wiley, New York, 1962), p. 531.
- [18] L. B. Hansen *et al.*, Mater. Sci. and Eng., in press.